When two's a crowd - Structural mapping of PEAK pseudokinase interactions identifies 14-3-3 as a molecular switch for PEAK3/Crk signaling.

Michael J. Roy[1,2,#], Minglyanna G. Surudoi[1,2], Ashleigh Kropp[1,2], Jianmei Hou[3,4,] Weiwen Dai[1,2], Joshua M. Hardy[1,2], Lung-Yu Liang[1,2], Thomas R. Cotton[1,2], Bernhard C. Lechtenberg[1,2], Toby A. Dite[1,2], Xiuquan Ma[3,4], Roger J. Daly[3,4], Onisha Patel[1,2*] and Isabelle S. Lucet[1,2,*,#]

[1.] The Walter and Eliza Hall Institute of Medical Research, Parkville, VIC 3052, Australia.

[2.] Department of Medical Biology, University of Melbourne, Parkville, VIC 3052, Australia.

[3.] Cancer Program, Biomedicine Discovery Institute, Monash University, Melbourne, VIC 3800, Australia.

[4.] Department of Biochemistry and Molecular Biology, Monash University, Melbourne, VIC 3800, Australia.

[*] Co-last authors

[#]Correspondence: roy@wehi.edu.au, lucet.i@wehi.edu.au,

Online content

Methods

PEAK Multiple Sequence Alignment (MSA) and SLiM analysis

Vertebrate orthologs of human PEAK-family proteins (PEAK3, PEAK1 and PEAK2/PRAG1) were compiled from the NBCI Gene database[1] (calculated by NCBI's Eukaryotic Genome Annotation pipeline) and manually curated to remove sequences annotated by NCBI as low quality. This yielded orthologs for PEAK3 (149 vertebrate orthologs), PEAK1 (301 vertebrate orthologs) and PEAK2 (206 vertebrate orthologs). Multiple Sequence Alignment for each set of PEAK orthologs and for the full family of all PEAK orthologs was performed using PROMALS3D[2] and visualized by web logo generation using WebLogo3[3]. Short Linear Motif (SLiM) analysis was performed using the Eukaryotic Linear Motif (ELM) server[4] and Scansite 4.0[5] and manual annotation.

Synthetic peptides and commercial recombinant protein

All synthetic peptides were purchased from Mimotopes (95% purity).

Proline rich motif peptides. 13-mer peptides encompassing proline-rich motifs from PEAK proteins were synthesized: PEAK3$^{54\text{-}66}$ (Ac-PLPPPLPKKILTR-NH2); PEAK1$^{1117\text{-}1129}$ (Ac-MIPPKQPRQPKGA-NH2); PEAK1$^{1150\text{-}1162}$ (Ac-PTPPPLPKKMIIR-NH2); PEAK2$^{709\text{-}721}$ (Ac-FSPPPPPPKSRHL-NH2); and PEAK2$^{809\text{-}821}$ (Ac-QPPPLPQKKIVSR-NH2).

SH2 peptides. A 7-mer sequence containing the putative Grb2/CrkII SH2 binding motif is common to both human PEAK3 (residues 23-29) and human PEAK1 (residues 1106-1112). Two synthetic 7mer peptides corresponding to this sequence were synthesized, either phosphorylated or non-phosphorylated at the tyrosine residue (PEAK SH2-pY peptide, Ac-T(pY)SNLGQ-NH2; and Ac-TYSNLGQ-NH2; both N-terminal acetylated, C-terminally amidated)[6].

Tandem peptides. Tandem peptides (phosphorylated and non-phosphorylated at the bolded/underlined residue) were also synthesized: PEAK3^{tandem} and PEAK3^{tandem}-pS69 (residues 54-74; Ac-PLPPPLPKKILTRTQ**S**LPTRR-NH2); PEAK1^{tandem} and PEAK1^{tandem}-pT1165 (residues 1152-1171; Ac-PPPLPKKMIIRAN**T**EPISKD-NH2); and PEAK2^{tandem} and PEAK2^{tandem}-pS826 (residues 812-831; Ac-PPPLPQKKIVSRAA**S**SPDGF-NH2).

Protein production of His-tagged adapter/scaffold proteins

Human gene sequences of adapter/scaffold proteins (full length or truncated versions) were codon optimized for *E. coli* expression and cloned into a pCOLD-IV vector (Takara) modified to encode an N-terminal 8-His tag and tobacco etch virus (TEV) protease cleavage site for tag removal. Several constructs were generated for this study. For adapter proteins this included: full length Grb2 (Grb2^{FL}; UniProt P62993-1, residues 1-217); full length CrkII (CrkII^{FL}; UniProt P46108-1, residues 1-330), and truncated forms of CrkII, including a SH2-NSH3 domain construct lacking the CSH3 domain (CrkII$^{\Delta CSH3}$ residues 1-228) and constructs of the individual CrkII SH2 domain (CrkII^{SH2}; UniProt P46108-1, residues 6-120) and CrkII NSH3 domain (CrkII^{NSH3}; UniProt P46108-1, residues 134-191). For 14-3-3 isoforms this included: 14-3-3ε (UniProt P62258-1; residues 1-255), 14-3-3η (UniProt Q04917-1; residues 1-246), 14-3-3γ (UniProt P61981-1; residues 1-247) and 14-3-3ς (UniProt P63104-1; residues 1-245). All constructs were verified using Sanger Sequencing (Micromon). Expressions were carried out overnight at 16°C for 16 to 20 hours in *E. coli* C41 (DE3) and proteins were purified using nickel affinity chromatography and size exclusion chromatography (SEC). When required, the His-tagged protein was cleaved following SEC with TEV protease. Cleaved samples were further purified by ion exchange chromatography (IEX) using Mono Q™ 5/50

GL (CrkII^{FL}, 14-3-3 and Grb2^{FL}) columns (Cytiva) (Extended Data Table 1). All protein samples were concentrated, flash frozen and stored at -80°C.

Protein production of PEAK proteins

Human PEAK1 (PEAK1^{IDR1}; UniProt Q9H792, residues 1082-1746), PEAK2 (PEAK2^{IDR1}; UniProt Q86YV5, residues 802-1406) and PEAK3 (PEAK3^{FL}; UniProt Q6ZS72, residues 1-473) were codon optimized for insect cell expression and cloned into a modified pFastBac™ Dual vector containing a N-terminal TEV cleavable His-tag under the polyhedrin promoter[7]. Expression was carried out in *Spodoptera frugiperda* (*Sf*21) cells and purification was performed as previously described[7] (Extended Data Table 2). Briefly, cell lysates were clarified by centrifugation at 45,500 x g for 1 hour at 4 °C and mixed with 0.5% (v/v) of His-tag purification resin (Roche) for purification by nickel affinity chromatography, PEAK proteins were further purified by SEC (HiLoad 16/600 Superdex 200 pg column). For PEAK3^{FL}, the resulting sample contained a mixture of PEAK3 protein in complex with two proteins identified by mass spectrometry as endogenous insect cell-derived 14-3-3ζ and 14-3-3ε (Extended Data Fig. 4a). PEAK1^{IDR1} and the PEAK3^{FL}:14-3-3ε,ζ complex were further purified by IEX (Mono Q™ 5/50 GL column). PEAK1^{IDR1}, PEAK2^{IDR1} and the PEAK3^{FL}: 14-3-3ε,ζ complex were concentrated to ~ 5 mg ml^{-1} and flash frozen in liquid nitrogen for subsequent studies.

Recombinant kinase domains for *in vitro* phosphorylation reactions

Constructs for expression of recombinant Src kinase domain (UniProt P12931, residues 254-536; Addgene plasmid #79700), Abl kinase domain (UniProt P00519-1, residues 229-512; Addgene plasmid #78173) and untagged YopH phosphatase (UniProt P08538-1, residues 164-468; Addgene plasmid #79749) from the Human Kinase Domain Constructs Kit for Automated Bacterial Expression (Addgene plasmid kit #1000000094) were a gift from John Chodera (Memorial Sloan Kettering Cancer Center)[8]. Co-expressions of Src/YopH or Abl/YopH were carried out overnight at 16°C for 16 to 20 hours in *E. coli* C41 (DE3) or *E. coli* Rosetta (DE3), respectively and purified as described using nickel affinity chromatography and SEC, without cleavage of the His-tag. Purified Abl kinase domain was stored at 2 mg ml^{-1} in 20 mM Tris pH 7.5, 150 mM NaCl, 5% glycerol, 0.5 mM TCEP. The Src kinase domain was further purified by IEX (Mono Q™ 5/50 GL column) and stored at 12 mg ml^{-1} in 20 mM Tris pH 8.0, 165 mM NaCl, 1 mM TCEP for subsequent studies (Extended Data Table 3).

Complex studies using analytical SEC and SEC-MALS

SEC analysis of protein complexes. SEC analysis of PEAK3^{FL}, PEAK2^{IDR1}, PEAK1^{IDR1} and CrkII^{FL} dimer/monomer (Fig. 3-4 and Extended Data Fig. 3) were performed on a Superdex^{TM} 200 Increase 10/300 GL (GE Healthcare) equilibrated in 20 mM HEPES pH 7.5-8.5, 150 mM NaCl, 1 mM TCEP. For individual analysis, PEAK and CrkII proteins were prepared at 20-50 μM concentration in a total volume of 110 μl. For complex interaction studies, in general PEAK and CrkII proteins were mixed at a 1:1-2 molar ratio (20-50 μM final concentration) in a total reaction volume of 110 μl, and the complex pre-equilibrated at room temperature for 25 min and filtered prior to SEC analysis. Elution peak fractions were analyzed by SDS-PAGE and peak elution fractions were pooled and concentrated and flash frozen in liquid nitrogen for subsequent studies.

SEC-MALS analysis of protein complexes. SEC multi-angle light scattering (SEC-MALS) experiments were performed using a Superdex 200 Increase 10/300 GL column (Cytiva) coupled with a DAWN HELEOS II light scattering detector and an Optilab TrEX refractive index detector (Wyatt Technology). The system was equilibrated in 20 mM HEPES pH 7.5, 150 mM NaCl, 1 mM TCEP and calibrated using bovine serum albumin (2 mg ml^{-1}; Sigma) before analysis of experimental samples. For each experiment, 100 μl of purified pre-equilibrated protein complex (120 μg of PEAK3^{FL}: 14-3-3ε,ζ and 170 μg of PEAK2^{IDR1}:CrkII^{FL} dimer) was injected onto the column and eluted at a flow rate of 0.5 ml min^{-1}. Experimental data were collected and processed using ASTRA software (Wyatt Technology, v.7.3.19).

Mass spectrometry (MS)

Tryptic MS phosphosite analysis of recombinant PEAK proteins. Recombinant purified PEAK1^{IDR1}, PEAK2^{IDR1} and PEAK3^{FL} were reduced with DTT (Sigma), carbamidomethylated with iodoacetamide (Sigma), and digested with trypsin (Promega). Prior to MS, the peptides were further purified and enriched using OMIX C18 Mini-Bed tips (Agilent Technologies). Using a Dionex UltiMate 3000 RSLCnano system equipped with a Dionex UltiMate 3000 RS autosampler, an Acclaim PepMap RSLC analytical column (75 μm × 50 cm, nanoViper, C18, 2 μm, 100 Å; Thermo Fisher Scientific), and an Acclaim PepMap 100 trap column (100 μm × 2 cm, nanoViper, C18, 5 μm, 100 Å; Thermo Fisher Scientific), the tryptic peptides were separated by increasing concentrations of 0.1% (v/v) formic acid (prepared in 80% (v/v) acetonitrile) at a flow rate of 250 nl min^{-1} for 50 min and analyzed with a QExactive HF mass spectrometer (Thermo Fisher Scientific).

To obtain peptide and phosphopeptide sequence information, the raw files were searched with Byonic (Protein Metrics, v. 3.1.0) against a human database obtained from UniProt (UP000005640) with the following parameters: carbamidomethylation at cysteine residues was specified as a fixed modification; oxidation at methionine residues and phosphorylation at serine, threonine, or tyrosine

residues were set as variable modifications; cleavage site specificity was set at C-terminal residues K and R with semi-specific cleavage specificity with up to two missed cleavages permitted; and precursor and fragment ion mass tolerances were set to 20 ppm. Only peptides identified within a false discovery rate of 1% based on a decoy database were reported.

In vitro ABL/SRC phosphorylation of PEAKs, CrkII and PTM analysis using tandem MS/MS. Phosphorylation reactions – Purified recombinant PEAK3^{FL} and PEAK1^{IDR1}, CrkII^{FL} were phosphorylated *in vitro* using recombinant Abl and Src. Substrate proteins were incubated at room temperature for 3 hours with recombinant Abl or Src kinase domains (5:1 molar ratio of substrate to kinase, 100 µl reaction volume) in 40 mM Tris pH 8.0, 150 mM NaCl, 10 mM MgCl2, 1 mM DTT and 5 mM ATP. Reactions were stopped with 25 mM EDTA. Control samples (no Abl or Src added to reaction) were performed analogously and included in MS analysis. MS analysis was performed as for recombinant PEAK proteins. Peptide and phosphopeptide sequences were obtained in Byonic using the same parameters as the tryptic MS phosphosite analysis.

Protein crystallization, data collection and processing

Grb2^{FL}:PEAK SH2-pY peptide complex. Crystallization of the Grb2^{FL}:PEAK SH2-pY peptide complex was accomplished based on the previously described method for Grb2^{FL} alone[9], using the hanging-drop vapor diffusion method at 20°C, and initial crystals optimized by varying pH, streak seeding and adjusting the drop ratio. The protein complex was prepared by concentrating Grb2^{FL} to 16 mg ml^{-1} with 1 mM peptide (diluted from 10 mM stock in water). Crystals used for data collection were obtained in 2.6 M sodium acetate pH 8.0, by mixing the protein/peptide complex with the well solution in a 2:1 ratio. Crystals were cryo-protected in 2.7 M sodium acetate pH 8.0, 10 % (v/v) glycerol, supplemented with 1 mM peptide and flash-frozen in liquid nitrogen. Diffraction data were collected on beamline MX2 at the Australian Synchrotron[10] using a wavelength of 0.9537 Å. Data were integrated by using XDS (v. 20161205)[11], scaled by using XSCALE (v. 20161205), and merged using AIMLESS (v. 0.5.21)[12,13]. The crystals belonged to space group $P\,4_3$ with unit cell parameters a = b = 89.0, c = 94.5 Å and α = β = γ = 90°, and contained two copies of Grb2^{FL} per asymmetric unit as a closely packed homodimer. The structure was solved by molecular replacement using PHASER (v. 2.8.3)[14] with Grb2^{FL} monomer coordinates derived from the existing Grb2^{FL} structure (PDB entry 1GRI) as the initial search model. Clear unbiased density was observed for the phosphopeptide in the SH2 phosphotyrosine binding site for one copy of Grb2^{FL} in the dimer, whilst no additional density was observed in the SH2 site in the second copy, which appeared to be occluded due to crystal packing. Iterative model building and refinement were performed in COOT (v. 0.9.8.1)[15] and PHENIX (v. 1.20.1-4487)[16], respectively, including a simulated annealing step in the first round of

refinement to minimize model bias and manual building of the phosphopeptide. The structure was refined to Rwork and Rfree values of 16.6% and 20.9%, respectively, with all of the residues in Ramachandran allowed regions as validated by MOLPROBITY[17]. The overall structure aligns closely with the earlier published structure for $Grb2^{FL}$ alone (PDB entry 1GRI, 3.1 Å resolution), with the addition of the PEAK1/3 pY-site phosphopeptide and some additional $Grb2^{FL}$ residues able to be modelled due to the higher resolution (2.3 Å resolution).

14-3-3ε:PEAK3^{tandem}-pS69 complex. The 14-3-3ε:PEAK3^{tandem}-pS69 peptide complex was prepared by incubating 14-3-3ε (10 mg ml^{-1} final concentration) with the PEAK tandem peptide (0.5 mM final concentration, diluted from 10 mM stock in water), representing a 1.5-fold molar excess of peptide. The complex was subjected to sparse matrix screening in a 96-well plate using the sitting-drop vapor diffusion method at 20°C and a 1:1 drop ratio of protein and well solution. Diffracting crystals were obtained in 2 M ammonium sulfate, 0.1 M sodium bicine pH 9.35, and 5% (v/v) 2-methyl-2,4,-pentandiol (MPD). Crystals were cryo-protected in 2.2 M ammonium sulfate, 0.02 M sodium bicine pH 9.35, 5% (v/v) MPD, and 20% (v/v) ethylene glycol supplemented with 100 μM peptide and flash-frozen in liquid nitrogen. Data collection and processing was performed as for the $Grb2^{FL}$:PEAK SH2-pY peptide complex. The crystals belonged to space group P 4_3 with unit cell parameters a = b = 155.42, c = 58.0 Å and α = β = γ = 90°, and contained four copies of 14-3-3ε monomer per asymmetric unit, arranged as two symmetrical homodimers as anticipated. Molecular replacement, model building and refinement were performed as for the $Grb2^{FL}$:PEAK SH2-pY peptide complex except that the human 14-3-3ε monomer structure (PDB entry 2BR9) was used as the initial search model. Clear unbiased density was observed for the phosphopeptide in the binding site of each 14-3-3ε monomer, although chain A showed the clearest resolved density following building and refinement. The structure was refined to Rwork and Rfree values of 18.7% and 23.3%, respectively, with 99.9% of the residues in Ramachandran allowed regions as validated by MOLPROBITY[17].

14-3-3ε:PEAK1^{tandem}-pT1165 complex. The structure of the 14-3-3ε:PEAK1^{tandem}-pT1165 complex was obtained by firstly crystallizing 14-3-3ε alone and then soaking the crystals with the PEAK tandem phosphopeptide. Successful conditions identified for the 14-3-3ε:PEAK3^{tandem}-pS69 peptide complex were used as the basis for 14-3-3ε crystallization trials using the hanging-drop vapor diffusion method at 20°C. Crystals of 14-3-3ε (10 mg ml^{-1}) were obtained in 1.8 M ammonium sulfate, 0.1 M HEPES pH 7.5, 5% (v/v) MPD, then transferred to well solution supplemented with 0.5 mM phosphopeptide to soak overnight. Crystals were cryo-protected in 2.2 M ammonium sulfate, 0.1 M HEPES pH 7.5, 5% (v/v) MPD, 20% (v/v) ethylene glycol supplemented with 0.5 mM phosphopeptide and flash-frozen in liquid nitrogen. Data collection, molecular replacement, and

model building and refinement were performed as for the 14-3-3ε:PEAK3^{tandem}-pS69 complex. The crystals belonged to space group *P* 6_2 2 2 with unit cell parameters a = b = 91.4, c = 139.9 Å and α = β = 90°, γ = 120° and contained one 14-3-3ε monomer per asymmetric unit. This particular crystal form represents a close crystal packing of 14-3-3ε as a monomer, in which residues 1-32 that would typically mediate the 14-3-3ε dimer interface are not resolved, as the crystal packing would require them to be at least partially unfolded. The remainder of the 14-3-3ε protein core aligns closely with the structure of dimeric 14-3-3ε (as for the 14-3-3ε*:PEAK3^{tandem}-pS69 complex*). Notably, the peptide binding groove is accessible and amenable to soaking and clear unbiased density for the PEAK phosphopeptide was observed. The final structure was refined to Rwork and Rfree values of 20.7% and 26.6%, respectively, with 99.5% of the residues in Ramachandran allowed regions as validated by MOLPROBITY[17].

14-3-3ε:PEAK2^{tandem}-pS826 complex. Crystallization, soaking, data collection and processing, and model building and refinement were performed identically as for the 14-3-3ε:PEAK1^{tandem}-pT1165 complex, but using the PEAK2^{tandem}-pS826 phosphopeptide. The crystals belonged to space group *P* 6_2 2 2 with unit cell parameters a = b = 92.1, c = 137.4 Å and α = β = 90°, γ = 120°, and contained one 14-3-3ε monomer per asymmetric unit, in the same close packing of the 14-3-3ε monomer. The final structure was refined to Rwork and Rfree values of 24.2% and 29.5%, respectively, with all the residues in Ramachandran allowed regions as validated by MOLPROBITY[17].

AlphaFold2 structure prediction of PEAK3^{FL} homodimer

The ColabFold Google Colab notebook called AlphaFold2_complexes[18,19] was used to predict the structure of dimeric human PEAK3^{FL}. The predicted model with the highest lDDT score is shown.

AlphaFold2 / HADDOCK analysis of SH2-pY motif

The PEAK3$^{23-27}$-pY^{24} peptide (T(pY)SNL) from the crystal structure of the Grb2^{FL}:PEAK SH2-pY peptide complex was spliced with the predicted structure of human PEAK3$^{28-38}$ (GQIRAHLLPSK) from the AlphaFold Protein Structure Database (EMBL-EBI)[20]. The spliced peptide was then docked into the Grb2^{FL} crystal structure using the HADDOCK server (v. 2.4)[21] and the highest ranked model was analyzed in ChimeraX (v. 1.4)[22] (Extended Data Fig. 2c, Fig. 2e).

Surface Plasmon Resonance (SPR) binding assays.

All SPR binding studies were performed using a Biacore S200 Instrument (Cytiva).

SPR binding studies to CrkII^{NSH3}. Purified CrkII^{NSH3} was diluted to 5 μg ml^{-1} in 10 mM sodium acetate pH 4.0 and amine coupled at 25°C to a Series S CM5 sensor chip, in HBS-N running buffer (20 mM

HEPES pH 7.4, 150 mM NaCl) to a final immobilization level of 1100-1400 response units (RU), followed by surface deactivation using 1 M ethanolamine. A blank activation/deactivation was used for the reference surface. Peptide binding studies were performed at 20°C in HBS-TP running buffer (20 mM HEPES pH 7.4, 150 mM NaCl, 1 mM TCEP, 0.005% (v/v) Tween-P20). Peptides were first prepared as 10 mM stocks in water: PEAK PRM peptides: PEAK3$^{54\text{-}66}$, PEAK1$^{1150\text{-}1162}$, PEAK2$^{709\text{-}721}$, PEAK2$^{809\text{-}821}$; or PEAK tandem motif peptides: PEAK3$^{\text{tandem, }54\text{-}74}$, PEAK3$^{\text{tandem, }54\text{-}74}$-pS69, PEAK1$^{\text{tandem, }1152\text{-}1171}$, PEAK1$^{\text{tandem, }1152\text{-}1171}$-pT1165, PEAK2$^{\text{tandem, }812\text{-}831}$, and PEAK2$^{\text{tandem, }812\text{-}831}$-pS826, phosphorylated or non-phosphorylated in the 14-3-3 motif. Peptide stocks were further diluted to in running buffer to 10 µM or 20 µM and prepared as a 11-point concentration series (2-fold serial dilution, 100 µM - 100 nM for PEAK PRM peptides, or 20 µM - 20 nM for PEAK tandem motif peptides). Samples were injected in a multi-cycle run (flow rate 30 µl min^{-1}, contact time of 60 seconds, dissociation 120 seconds) without regeneration. Sensorgrams were double referenced, and steady state binding data fitted using a 1:1 binding model using Biacore S200 Evaluation Software (Cytiva, v. 1.1). Representative sensorgrams and fitted dissociation constant (K_D) values, depicted as mean ± S.E.M. (N > 3 independent experiments) or mean ± S.D. (N = 2), are shown in Source Data Fig. 3.

SPR binding studies to 14-3-3 isoforms. Immobilization of 14-3-3 isoforms (14-3-3γ, 14-3-3ε, 14-3-3σ, and 14-3-3η; diluted to 10 µg ml^{-1} in 10 mM sodium acetate pH 4.0) was performed as described for CrkII^{NSH3} at 20°C to a final immobilization level 1800 – 2900 RU. Binding studies were run using PEAK tandem peptides (11-point concentration series, 2-fold serial dilution; 10 µM - 10 nM for PEAK3^{tandem}-pS69, 20 µM – 20 nM for all other peptides). SPR binding experiments and steady state data analysis were performed as described for CrkII^{NSH3}. Representative sensorgrams and fitted dissociation constant (K_D) values, depicted as mean ± S.E.M. (N > 3 independent experiments), are shown in Source Data SPR Fig.4.

Isothermal Titration Calorimetry (ITC) binding experiments and cooperativity analysis.

ITC binding experiments were conducted using a MicroCal iTC200 instrument (Malvern Instruments). Titrations were conducted at 25 °C in reverse mode (peptide in cell, protein in syringe) and consisted of 19 injections of 2 µL peptide solution at a rate of 2 sec µL^{-1} at 90 sec time intervals, whilst stirring at 1000 rpm. An initial injection of 0.4 µL protein was made and discarded during data analysis. Proteins (14-3-3ɣ or CrkII^{NSH3}) were first dialyzed overnight at 4°C into ITC buffer (20 mM HEPES pH 7.4, 150 mM NaCl, 1 mM TCEP), filtered and degassed under vacuum. Peptides (PEAK3^{tandem} or PEAK3^{tandem}pS69) were diluted into filtered, degassed ITC buffer from 10 mM stock solutions prepared in water. For the binary experiment of CrkII^{NSH3} binding to PEAK3^{tandem} peptide,

CrkII^{NSH3} (140 μM, in the syringe) was titrated into PEAK3^{tandem} peptide (20 μM, in the cell). For binding studies to examine cooperativity, sequential ITC titrations were performed according to the following general procedure: In the first titration (binary), 14-3-3ɣ (200 μM, in the syringe) or a buffer control were titrated into PEAK3^{tandem} or PEAK3^{tandem}pS69 peptide (20 μM, in the cell). Following the first titration, excess solution was removed from the cell, and the syringe was washed and dried. In the second titration (ternary), CrkII^{NSH3} (400 μM, in the syringe) was titrated into the peptide complex remaining in the cell (16.8 μM). The concentration of saturated peptide complex in the cell (C) after the first titration (16.8 μM), was calculated using the equation: $C = (C_0 \cdot V_{cell})/(V_{cell}+V_{inj})$ where C_0 is the initial peptide concentration (20 μM), V_{cell} is the volume of the cell (200.1 μl) and V_{inj} is the volume of titrant injected during the first titration (38.4 μl). All data were fitted to a single binding site model to obtain the stoichiometry (N), the dissociation constant (K_D) and the enthalpy of binding (ΔH), using Microcal Origin (OriginLab, v. 7.0). The reported values are the mean ± S.E.M. (N > 3) from independent measurements (Extended Data Fig. 6).

Cellular studies of PEAK interactions (HEK293 cells)

Antibodies and tissue culture. The following antibodies were obtained commercially: anti-HA (Cell Signaling Technology, catalog no. 3724), anti-Flag (Sigma-Aldrich, catalog no. F1804), anti-14–3-3 (Santa Cruz Biotechnology, catalog no. sc-1657) and anti-CrkII (Santa Cruz Biotechnology, catalog no. sc-289). HEK293 cells were maintained as previously described[6].

Plasmids. Codon-optimized cDNAs encoding N-terminal HA-tagged or Flag-tagged WT PEAK3^{FL} and HA-tagged PEAK3^{FL} mutants were synthesized as previously described[6]. Plasmid transfections in HEK293 cells were performed using Lipofectamine 3000 (Life Technologies, catalog no. L3000015) according to the manufacturer's instructions.

Cell lysis and immunoprecipitation. Control HEK293 cells or HEK293 cells singly expressing HA-tagged PEAK3^{FL} WT or HA-tagged PEAK3^{FL}-S69A mutant, or co-expressing Flag-tagged PEAK3^{FL} WT with various HA-tagged PEAK3^{FL} dimerisation mutants (PEAK3^{FL}-S69A, -L146E, -A436E, or -C453E) were harvested after 48h post transfection. Cell lysates for co-immunoprecipitation were prepared using standard lysis buffers[23]. Cell lysates were incubated with anti-HA affinity-agarose beads (Sigma-Aldrich, catalog no. E6679) at 4°C overnight on a shaking platform. After extensive washing with ice-cold lysis buffer, the immune complexes were eluted with SDS–polyacrylamide gel electrophoresis loading buffer and subjected to Western blotting analysis. Uncropped gels can be found in Source data.

References

1. Sayers, E.W. et al. Database resources of the national center for biotechnology information. *Nucleic Acids Res* **50**, D20-D26 (2022).
2. Pei, J., Tang, M. & Grishin, N.V. PROMALS3D web server for accurate multiple protein sequence and structure alignments. *Nucleic Acids Res* **36**, W30-4 (2008).
3. Crooks, G.E., Hon, G., Chandonia, J.M. & Brenner, S.E. WebLogo: a sequence logo generator. *Genome Res* **14**, 1188-90 (2004).
4. Kumar, M. et al. The Eukaryotic Linear Motif resource: 2022 release. *Nucleic Acids Res* **50**, D497-D508 (2022).
5. Obenauer, J.C., Cantley, L.C. & Yaffe, M.B. Scansite 2.0: Proteome-wide prediction of cell signaling interactions using short sequence motifs. *Nucleic Acids Res* **31**, 3635-41 (2003).
6. Hou, J. et al. Distinct PEAK3 interactors and outputs expand the signaling potential of the PEAK pseudokinase family. *Sci Signal* **15**, eabj3554 (2022).
7. Patel, O. et al. Production and purification of the PEAK pseudokinases for structural and functional studies. *Methods Enzymol* **667**, 1-35 (2022).
8. Albanese, S.K. et al. An Open Library of Human Kinase Domain Constructs for Automated Bacterial Expression. *Biochemistry* **57**, 4675-4689 (2018).
9. Maignan, S. et al. Crystal structure of the mammalian Grb2 adaptor. *Science* **268**, 291-3 (1995).
10. Aragao, D. et al. MX2: a high-flux undulator microfocus beamline serving both the chemical and macromolecular crystallography communities at the Australian Synchrotron. *J Synchrotron Radiat* **25**, 885-891 (2018).
11. Kabsch, W. Xds. *Acta Crystallogr D Biol Crystallogr* **66**, 125-32 (2010).
12. Evans, P.R. & Murshudov, G.N. How good are my data and what is the resolution? *Acta Crystallogr D Biol Crystallogr* **69**, 1204-14 (2013).
13. Winn, M.D. et al. Overview of the CCP4 suite and current developments. *Acta Crystallogr D Biol Crystallogr* **67**, 235-42 (2011).
14. McCoy, A.J. et al. Phaser crystallographic software. *J Appl Crystallogr* **40**, 658-674 (2007).
15. Emsley, P. & Cowtan, K. Coot: model-building tools for molecular graphics. *Acta Crystallogr D Biol Crystallogr* **60**, 2126-32 (2004).
16. Afonine, P.V. et al. Towards automated crystallographic structure refinement with phenix.refine. *Acta Crystallogr D Biol Crystallogr* **68**, 352-67 (2012).
17. Chen, V.B. et al. MolProbity: all-atom structure validation for macromolecular crystallography. *Acta Crystallogr D Biol Crystallogr* **66**, 12-21 (2010).
18. Mirdita, M. et al. ColabFold: making protein folding accessible to all. *Nat Methods* **19**, 679-682 (2022).
19. Tunyasuvunakool, K. et al. Highly accurate protein structure prediction for the human proteome. *Nature* **596**, 590-596 (2021).
20. Jumper, J. et al. Highly accurate protein structure prediction with AlphaFold. *Nature* **596**, 583-589 (2021).
21. van Zundert, G.C.P. et al. The HADDOCK2.2 Web Server: User-Friendly Integrative Modeling of Biomolecular Complexes. *J Mol Biol* **428**, 720-725 (2016).
22. Pettersen, E.F. et al. UCSF ChimeraX: Structure visualization for researchers, educators, and developers. *Protein Sci* **30**, 70-82 (2021).
23. Brummer, T. et al. Increased proliferation and altered growth factor dependence of human mammary epithelial cells overexpressing the Gab2 docking protein. *J Biol Chem* **281**, 626-37 (2006).

Extended Data Table 1. Purification buffers for adaptor/scaffold proteins.

Buffers	**14-3-3 isoforms**	**CrkII^{FL}** **CrkII$^{\Delta CSH3}$** **CrkII^{NSH3}** **CrkII^{SH2}**	**Grb2^{FL}** **Grb2^{SH2}**
Lysis	20 mM Tris pH 7.5 500 mM NaCl 5 mM DTT 5 mM imidazole 10% (v/v) glycerol 0.1% (w/v) Thesit 2 mM EDTA	20 mM Tris pH 7.5 500 mM NaCl 5 mM DTT 5 mM imidazole 10% (v/v) glycerol 0.1% (w/v) Thesit	20 mM Tris pH 7.5 500 mM NaCl 5 mM DTT 5 mM imidazole 10% (v/v) glycerol 0.1% (w/v) Thesit
Ni-Affinity Wash	20 mM Tris pH 7.5 500 mM NaCl 5 mM DTT 5 mM imidazole 10% (v/v) glycerol 2 mM EDTA	20 mM Tris pH 7.5 500 mM NaCl 5 mM DTT 5 mM imidazole 10% (v/v) glycerol	20 mM Tris pH 7.5 500 mM NaCl 5 mM DTT 5 mM imidazole 10% (v/v) glycerol
Ni-Affinity Elution	Ni-Affinity Wash Buffer 250 mM imidazole	Ni-Affinity Wash Buffer 250 mM imidazole	Ni-Affinity Wash Buffer 250 mM imidazole
SEC	20 mM HEPES pH 7.5 150 mM NaCl 0.5 mM TCEP	20 mM Tris pH 7.5 200 mM NaCl 0.5 mM TCEP 5% (v/v) glycerol	20 mM Tris pH 7.5 200 mM NaCl 0.5 mM TCEP 5% (v/v) glycerol
IEX Buffer A	20 mM HEPES pH 7.5 0.5 mM TCEP	20 mM HEPES pH 7.5 0.5 mM TCEP	20 mM HEPES pH 7.5 0.5 mM TCEP 5% (v/v) glycerol
IEX Buffer B	20 mM HEPES pH 7.5 1 M NaCl 0.5 mM TCEP	20 mM HEPES pH 7.5 1 M NaCl 0.5 mM TCEP	20 mM HEPES pH 7.5 1 M NaCl 0.5 mM TCEP 5% (v/v) glycerol

Extended Data Table 2. Purification buffers for PEAK proteins.

Buffers	PEAK1^{IDR1}	PEAK2^{IDR1}	PEAK3^{FL}
Lysis	20 mM Tris pH 8.0 500 mM NaCl 5 mM DTT 10 mM imidazole 10% (v/v) glycerol 0.1% (w/v) Thesit 2 mM EDTA	20 mM Tris pH 8.5 500 mM NaCl 10 mM DTT 5 mM imidazole 10% (v/v) glycerol 0.1% (w/v) Thesit 2 mM EDTA	20 mM Tris pH 7.5 500mM NaCl 10 mM DTT 20 mM imidazole 10% (v/v) glycerol 0.1% (w/v) Thesit
Ni-Affinity Wash	20 mM Tris pH 8 500 mM NaCl 5 mM DTT 10 mM imidazole 10% (v/v) glycerol 2 mM EDTA	20 mM Tris pH 8.5 500 mM NaCl 10 mM DTT 5 mM imidazole 10% (v/v) glycerol 2 mM EDTA	20 mM Tris pH 7.5 500 mM NaCl 10 mM DTT 20 mM imidazole, 10% (v/v) glycerol
Ni-Affinity Elution	Ni-Affinity Wash Buffer 250 mM imidazole	Ni-Affinity Wash Buffer 250 mM imidazole	Ni-Affinity Wash Buffer 250 mM imidazole
SEC	20 mM Tris pH 8.0 200 mM NaCl 0.5 mM TCEP 5% (v/v) glycerol	20 mM Tris pH 8.5 200 mM NaCl 1 mM TCEP 5% (v/v) glycerol	20 mM Tris pH 7.5 250 mM NaCl 1 mM TCEP
IEX Buffer A	20 mM Tris pH 8.0 1 mM TCEP 5% (v/v) glycerol	N/A	20 mM Tris pH 7.5 1 mM TCEP
IEX Buffer B	20 mM Tris pH 8.0 1 M NaCl 1 mM TCEP 5% (v/v) glycerol	N/A	20 mM Tris pH 7.5 1 M NaCl 1 mM TCEP

Extended Data Table 3. Purification buffers for kinase domains for *in vitro* phosphorylation reactions.

Buffers	Src	Abl
Lysis	50 mM Tris pH 8.0 500 mM NaCl 1 mM DTT 10 mM imidazole 5% (v/v) glycerol 0.1% (w/v) Thesit	20 mM Tris pH 7.5 500 mM NaCl 5 mM DTT 5 mM imidazole 10% (v/v) glycerol 0.1% (w/v) Thesit
Ni-Affinity Wash	50 mM Tris pH 7.5 500 mM NaCl 1 mM DTT 25 mM imidazole 5% (v/v) glycerol	20 mM Tris pH 7.5 500 mM NaCl 5 mM DTT 5 mM imidazole 10% (v/v) glycerol
Ni-Affinity Elution	Ni-Affinity Wash Buffer 250 mM imidazole	Ni-Affinity Wash Buffer 250 mM imidazole
SEC	20 mM Tris pH 8.0 150 mM NaCl 1 mM DTT	20 mM Tris pH 7.5 150 mM NaCl 5% (v/v) glycerol 0.5 mM TCEP
IEX Buffer A	20 mM Tris pH 8.0 1 mM TCEP	N/A
IEX Buffer B	20 mM Tris pH 8.0 1 M NaCl 1 mM TCEP	N/A

Extended Data Figure Legends.

Extended Data Fig. 1. a, Full MSA/Web Logo of conservation across PEAK3/PEAK1/PEAK2 vertebrate orthologs (N-IDR1 region). **b,** Full MSA/Web Logo of PEAK3 orthologs (N-terminal IDR1 region). Regions of interest for this study are highlighted, in particular the conserved SH2 pY binding site present in PEAK3/PEAK1 (TYSNL motif) and the 'tandem site' (encompassing proline rich motif known to bind $CrkII^{NSH3}$ and putative 14-3-3 binding motif).

Extended Data Fig. 2. a-b, AlphaFold2 (AF2) structures of (a) $PEAK1^{1106-1121}$ and (b) $PEAK3^{23-38}$ regions alongside Full MSA/Web Logo of orthologs for the corresponding sequence, showing a section of high sequence conservation (pale yellow box) adjacent to the TYSNL SH2 site (yellow box, underlined) including a region predicted in AF2 to adopt helical secondary structure (red box). **c,** Workflow to generate HADDOCK docking model of extended $PEAK3^{23-38}$-pY^{24} peptide (TpYSNL motif and predicted helical region) bound to $Grb2^{FL}$.

Extended Data Fig. 3 a, Schematic highlighting synthetic peptides generated for PEAK1, PEAK2 or PEAK3 encompassing Proline Rich Motifs (PRMs) predicted to bind $CrkII^{NSH3}$ domain. **b,** Size exclusion chromatography (SEC) profile (S75 16/600) of $CrkII^{FL}$ and truncated $CrkII^{\Delta CSH3}$ and $CrkII^{SH2}$ constructs showing a similar proportion of dimer, indicating that the SH2 domain mediates dimerization. **c,** Overlaid SEC profiles (S200 10/300) of individually purified $CrkII^{FL}$ dimer and $CrkII^{FL}$ monomer. **d,** Incubation of $PEAK1^{IDR1}$ with $CrkII^{FL}$ dimer (1:1.3 molar ratio) results in formation of a stable complex, as analysed by SEC confirmed by SDS-PAGE analysis of eluted fractions. **e,** SEC-MALS analysis of $PEAK2^{IDR1}$ dimer:$CrkII^{FL}$ dimer complex and $PEAK2^{IDR1}$ dimer alone. Absorbance was measured at a wavelength of 280 nm. Theoretical and observed molecular mass values are indicated. A diagram of the $PEAK2^{IDR1}$ dimer:$CrkII^{FL}$ dimer complex is shown.

Extended Data Fig. 4: a, Table summarising phosphorylation state at the tandem site 14-3-3 motif as identified by LC MS/MS for recombinant PEAK proteins purified from insect cells. Mass-directed tryptic proteomics proteomic analysis identifying phosphorylation sites for recombinantly purified PEAK proteins, as well as identification of 14-3-3 isoforms in the purified $PEAK3^{FL}$:14-3-3 complex purified from insect cells are both available in source data. **b,** Western blot analysis for immunoprecipitation of HA-tagged $PEAK3^{FL}$ WT and $PEAK3^{FL}$ S69A expressed in HEK293 cells and probed using anti-HA, anti-14-3-3 and anti-CrkII; showing that the S69 site is required for 14-3-3 co-immunoprecipitation with $PEAK3^{FL}$ from cells and that mutation of this critical 14-3-3 site

(PEAK3^{FL} S69A mutant) is concomitant with a modest increase in the observed level of CrkII bound to PEAK3^{FL}. Densitometry data quantifying the mean level relative association of CrkII to HA-PEAK3^{FL} S69A relative to WT. Western blot and densitometry data represent three independent repeats; uncertainties are S.E.M; ** $p<0.01$, by ratio paired t-test. **c,** PEAK3 mutants (L146E, A436E, C453E) that disrupt dimerization reduce 14-3-3 interaction with PEAK3. Flag-tagged PEAK3 WT and HA-tagged PEAK3 WT or dimerization mutants were co-expressed in HEK293 cells. Anti-HA IPs were prepared from cell lysates and Western blotted as indicated. Data are representative of N=3 independent experiments.

Extended Data Fig. 5: a, Primary sequence of PEAK tandem peptides; phosphorylated or non-phosphorylated at the underlined residue (red). **b,** Comparison of crystal structures of PEAK tandem phosphopeptides with 14-3-3ε, showing PEAK1^{tandem}-pT1165 (top left, grey sticks), PEAK3^{tandem}-pS69 (top right, yellow sticks) and PEAK2^{tandem}-pS826 (bottom left, purple sticks) peptides bound to the groove of 14-3-3ε (maroon surface/cartoon) and overlay of all three PEAK peptides (bottom right) demonstrating phospho-recognition by 14-3-3. **c,** Heatmap of SPR steady state affinity values (K_D) of human 14-3-3 isoforms for phosphorylated PEAK tandem peptides (see Supplementary Information for tabulated SPR data).

Extended Data Fig. 6: a-d, Sequential ITC binding studies using PEAK3^{tandem}-S69 (non-phosphorylated, left, a/c) and PEAK3^{tandem}-pS69 (phosphorylated, right, b/d) peptides and purified 14-3-3ɣ and CrkII^{NSH3} domain. Corresponding ITC derived affinity values (K_D) (mean value, N > 1) and the number of independent experiments (N) are shown on the representative plot for each titration (see Supplementary Information for tabulated ITC data).

Extended Data Fig. 7: a, Schematic of PEAK signaling pathways at focal adhesions. **b,** Schematic summarizing the approximate binding affinity (K_D for 1:1 interaction) of Grb2, CrkII and 14-3-3 towards PEAK1/PEAK2/PEAK3 dimers at N-terminal IDR motifs examined in this study, highlighting PEAK homodimer and heterodimer configurations and diverse interaction outputs.

Extended data Fig. 1

a

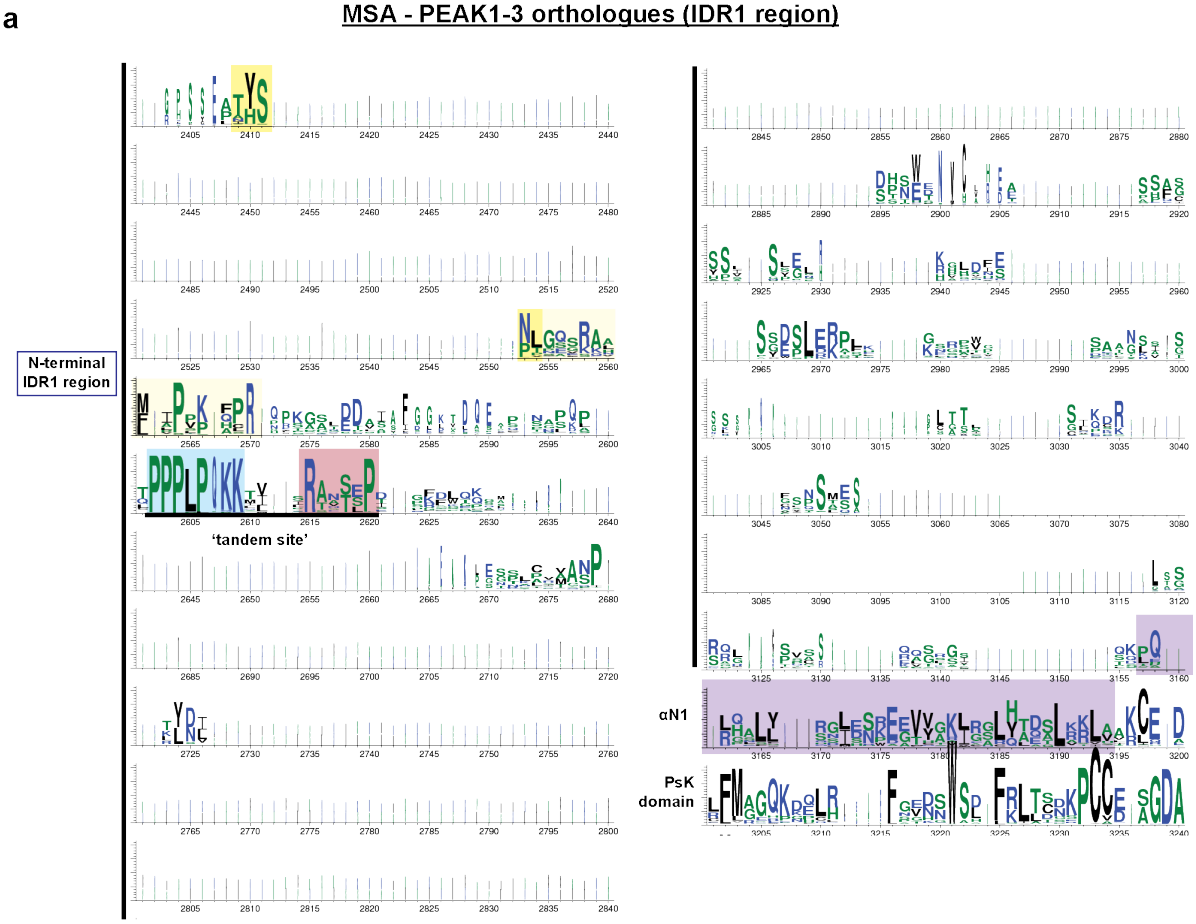

b

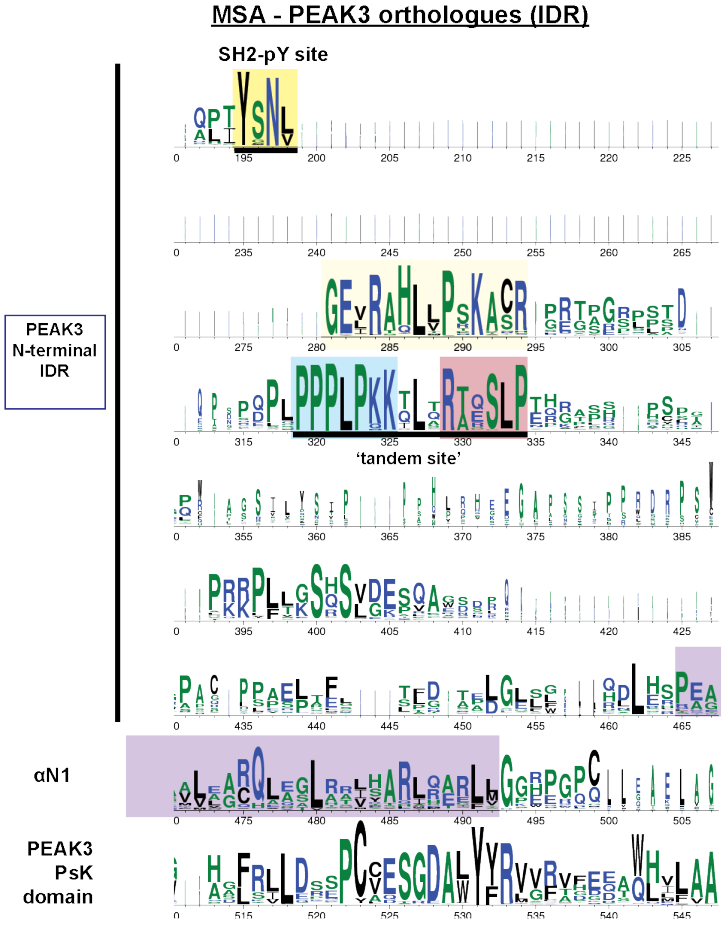

Extended Data Fig. 2

a MSA - PEAK3 orthologues

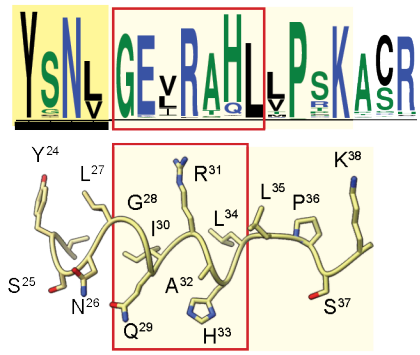

b MSA - PEAK1 orthologues

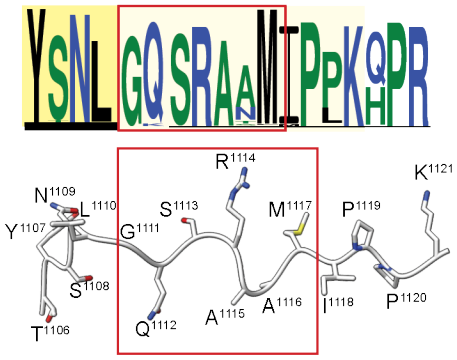

c

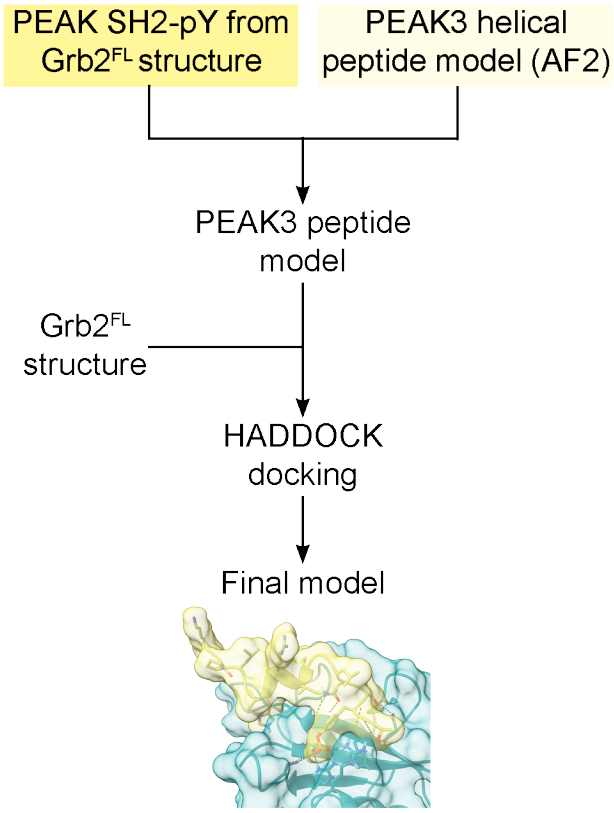

Extended Data Fig. 3

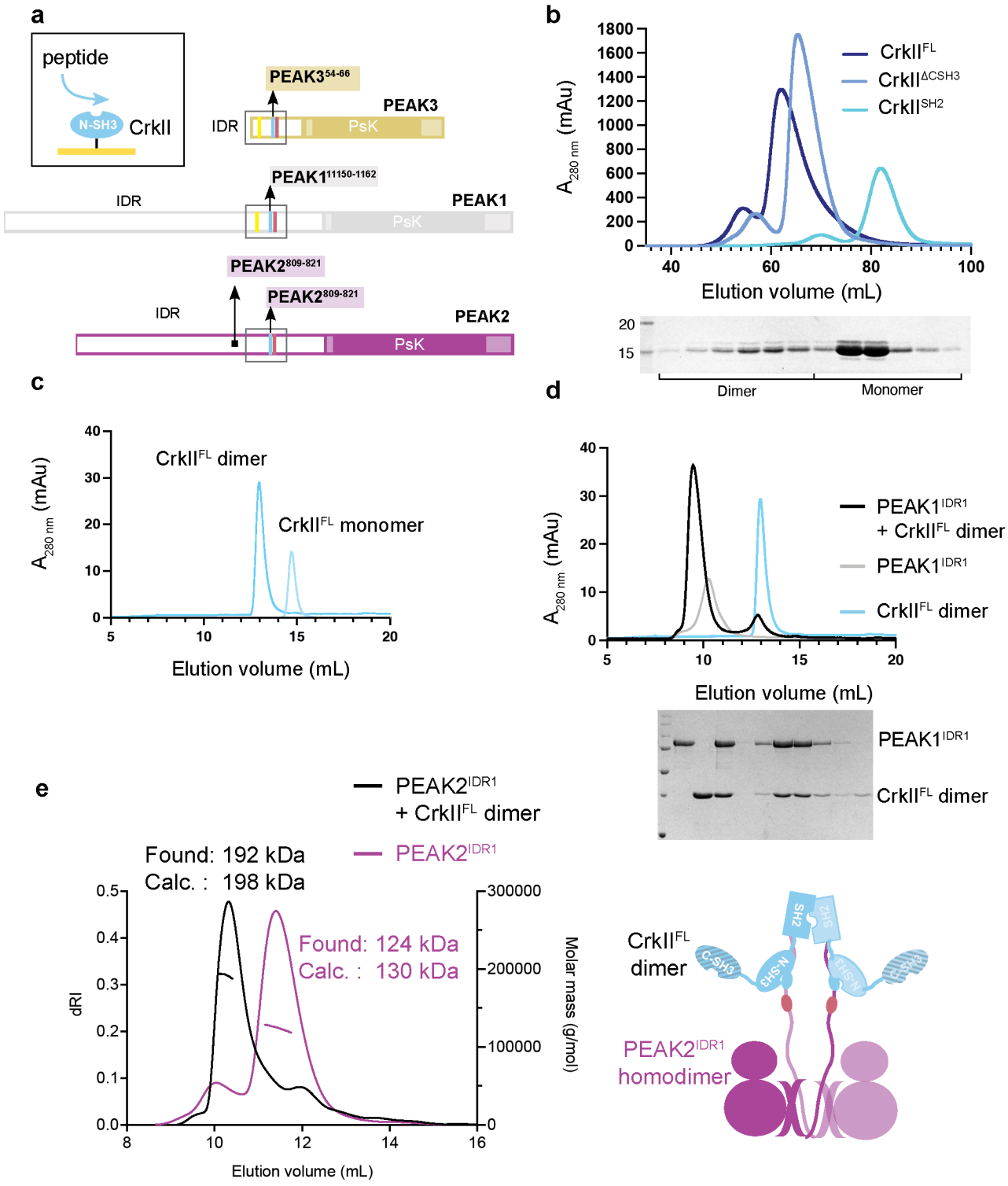

Extended Data Fig. 4

a

Protein (from *Sf.* 21 insect cells)	14-3-3 motif	14-3-3 motif phosphorylated (LC MS/MS)
PEAK3^{FL}	RTQ**S**LP	Y
PEAK1^{IDR1}	RANTEP	N
PEAK2^{IDR1}	RAA**S**SP	Y

b

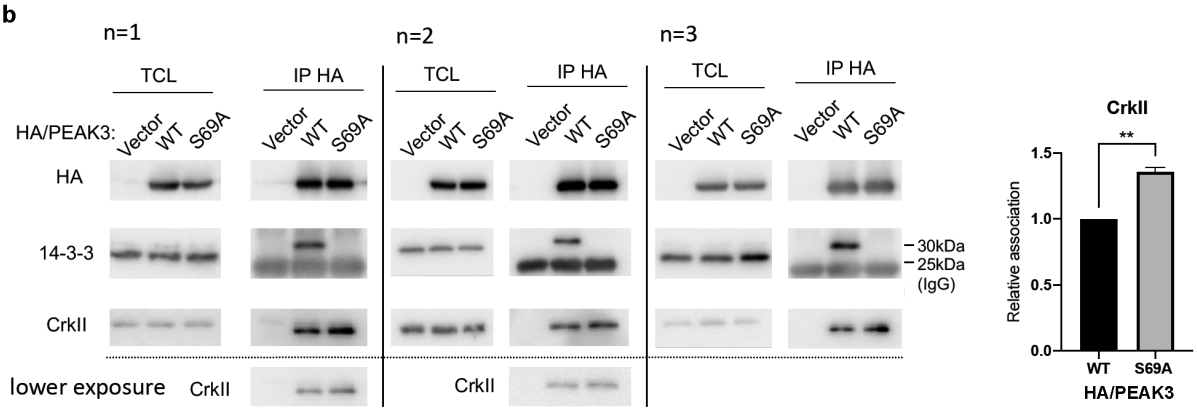

c

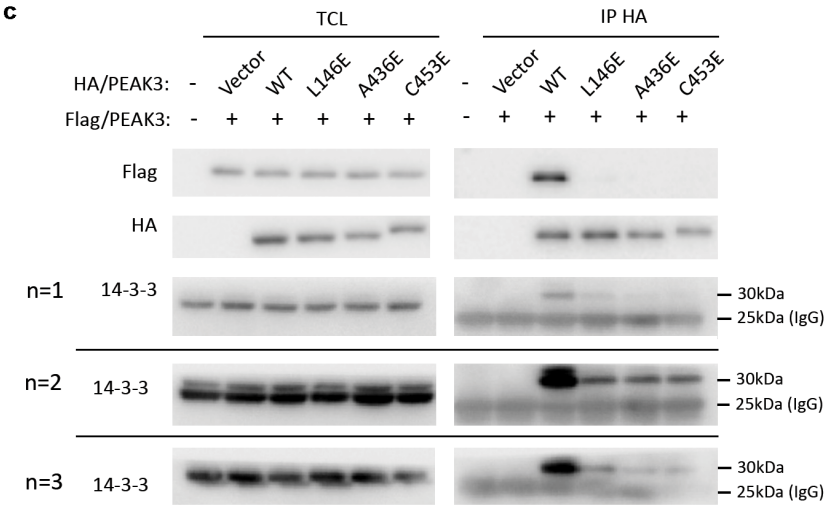

Extended Data Fig. 5

a

PEAK1^{tandem} peptide (1152-1171)	Ac-PPPLPKKMIIRANTEPISKD-NH2
PEAK2^{tandem} peptide (812-831)	Ac-PPPLPQKKIVSRAASSPDGF-NH2
PEAK3^{tandem} peptide (54-74)	Ac-PLPPPLPKKILTRTQSLPTRR-NH2

b

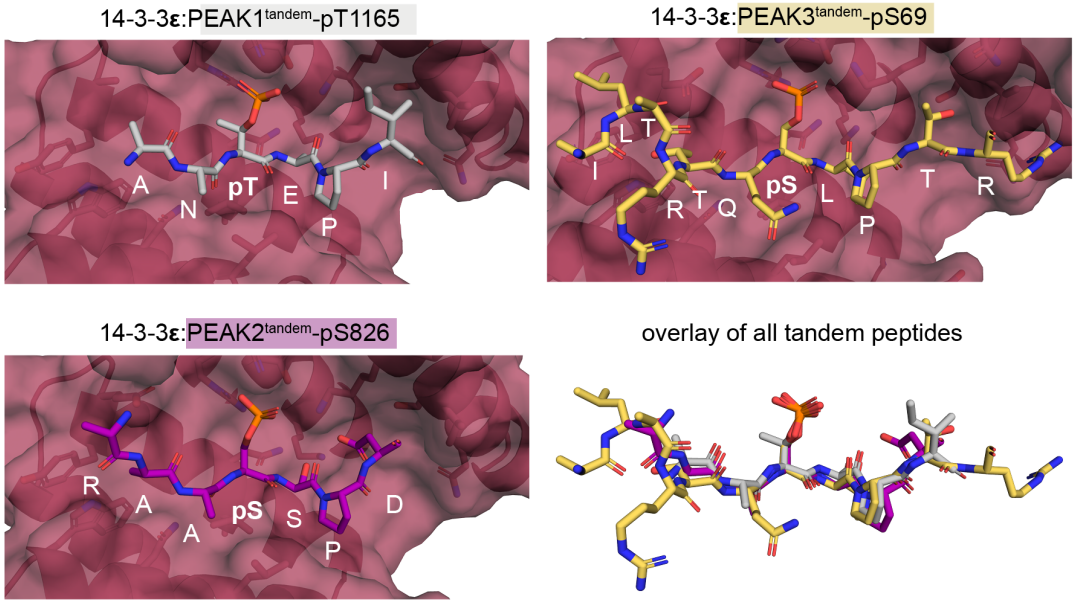

c

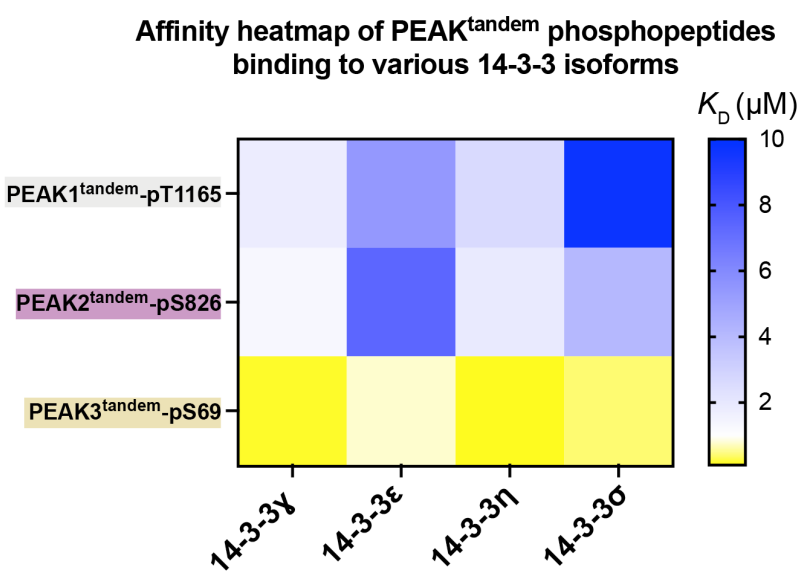

Extended Data Fig.6

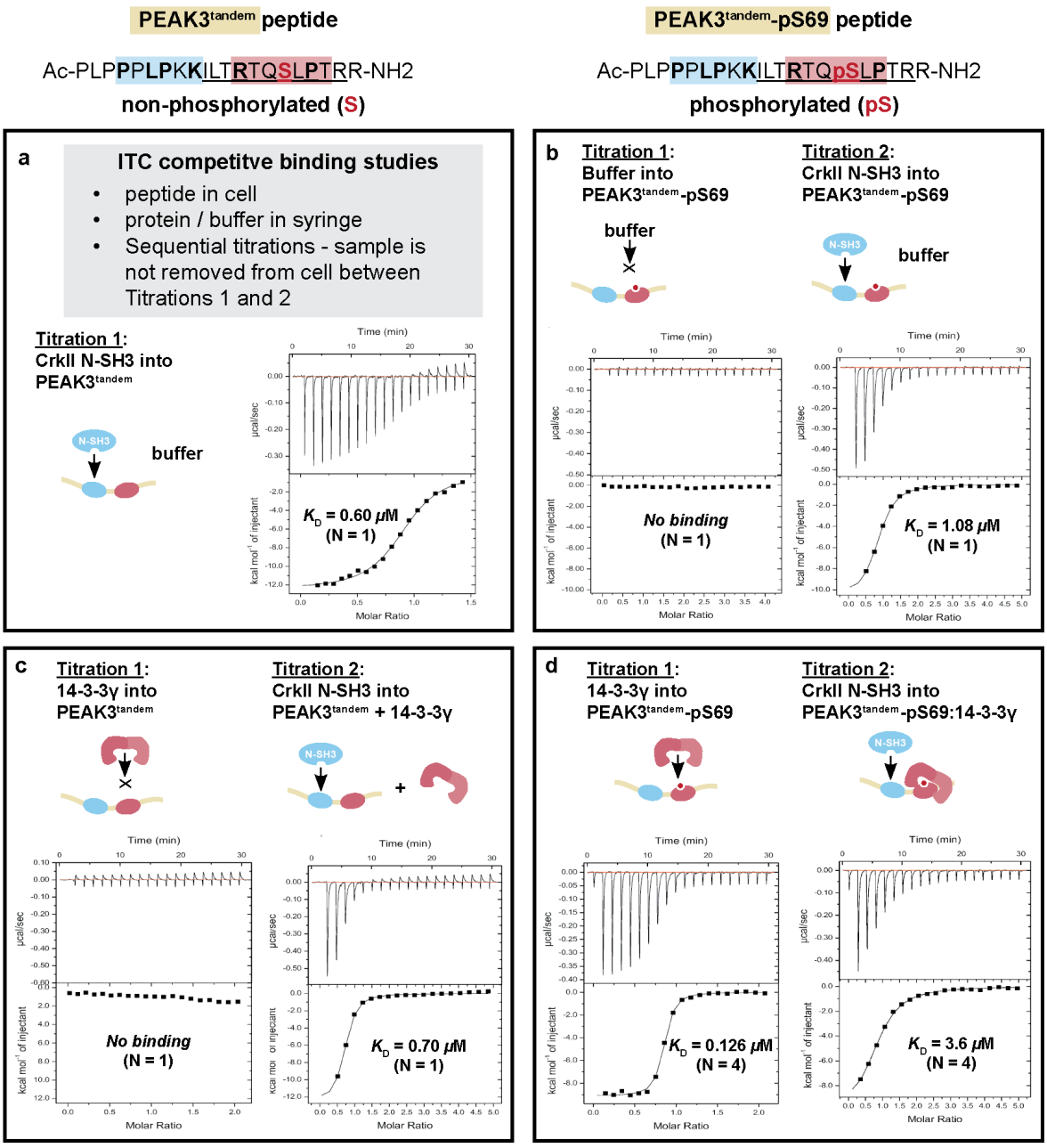

Fig. 7 Extended

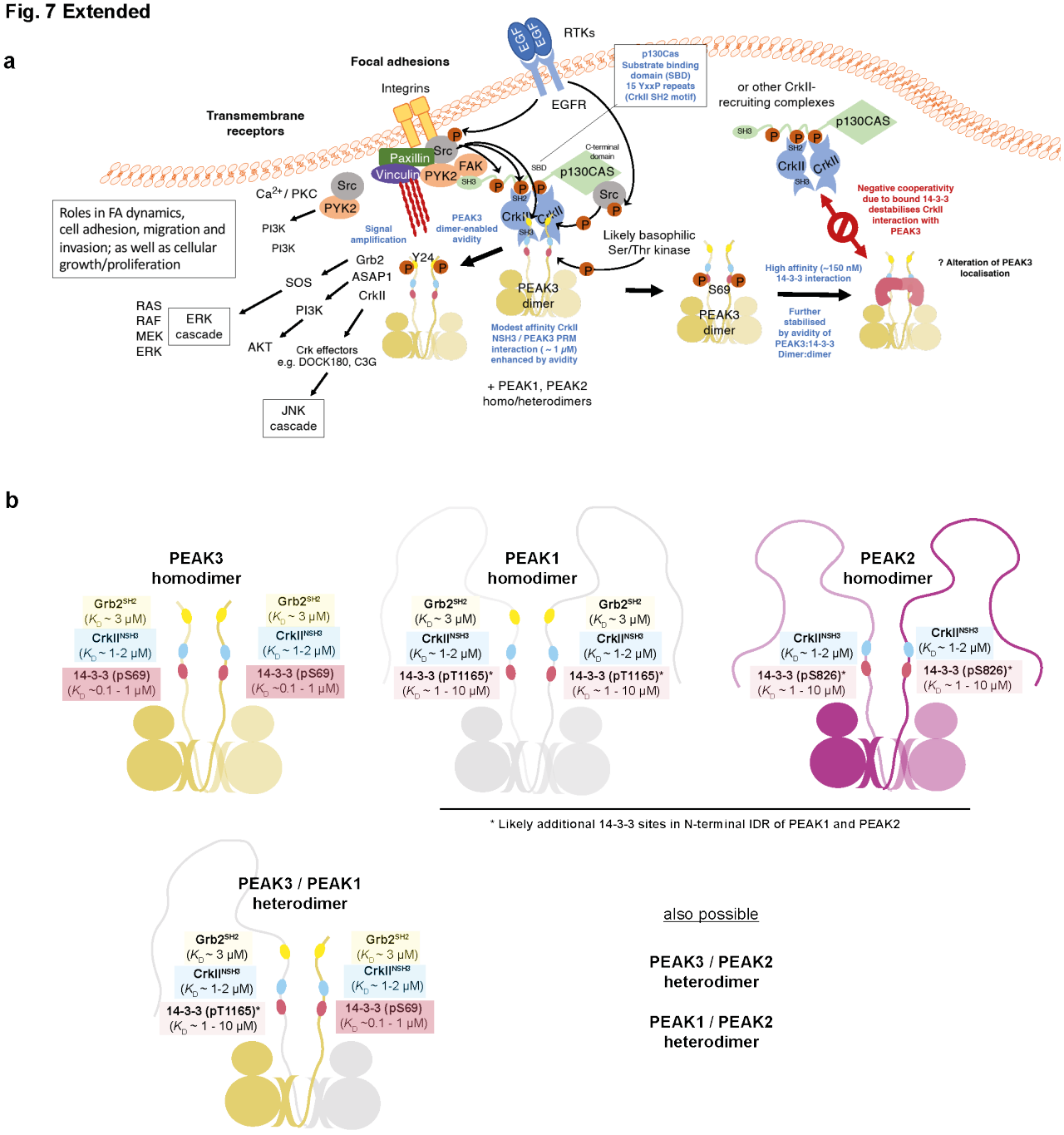

491

492